engineering proceedings

MDPI

Proceeding Paper

A Load Identification Method in Structural Design †

Giacomo Cangi [1,2,*,‡], Massimiliano Palmieri [1,‡] and Filippo Cianetti [1,‡]

[1] Department of Engineering, University of Perugia, Via G. Duranti 93, 06125 Perugia, Italy; massimiliano.palmieri@unipg.it (M.P.); filippo.cianetti@unipg.it (F.C.)
[2] Terex Italia S.R.L., Via Cassoletta, 76, 40056 Crespellano, Italy
* Correspondence: giacomo.cangi@dottorandi.unipg.it
† Presented at the 54th Conference of the Italian Scientific Society of Mechanical Engineering Design (AIAS 2025), Florence, Italy, 3–6 September 2025.
‡ These authors contributed equally to this work.

Abstract

One of the most critical aspects of design for an analyst or designer is understanding the service loads that a system or component will experience. In a standard finite element (FE) analysis, the service load history is applied to the FE model to generate the corresponding history of stresses and strains, which are necessary for further evaluations. However, for components operating in complex environments, accurately measuring or predicting the service load history can be particularly challenging. Instrumenting a prototype with load transducers is often an expensive and time-consuming process and, most importantly, may physically alter the component, changing its mass, stiffness, and load path, causing discrepancies between the measured and actual loads. In this context, this paper presents a load identification method, enhancing the methodology behind the load identification theory and reducing the uncertainties inherent in the standard approach, primarily due to the placement, number, and orientation of strain gauges.

Keywords: dynamics; structural dynamics; structural design

1. Introduction

Characterizing service loads is a critical aspect of engineering design, vibration control, structural health monitoring and seismic design [1]. For analysts, accurately defining these loads is fundamental to ensuring structural integrity and optimal performance from the earliest design stages [2]. In standard finite element (FE) analysis, service load histories are applied to FE models to compute stress and strain responses for subsequent evaluations [3]. Service load data can be obtained from three primary sources: established standards, which provide reference load cases or spectra for design verification and compliance; multi-body simulations, which predict dynamic loads by modeling component interactions under various operating scenarios [4,5]; and direct experimental measurements, which offer the most accurate representation of actual in-service conditions. When standards are inapplicable and simulations are infeasible due to model complexity or computational constraints, direct measurement remains the only viable option. However, directly measuring service loads on components in complex environments is particularly challenging. Loading conditions are often variable, multi-axial, and influenced by unpredictable operational and environmental factors. Consequently, the fidelity of FE analysis and the resulting design reliability heavily depend on the quality of the input load data. Direct measurement is often impractical due to several limitations: limited physical accessibility to critical points, structural alterations

Academic Editors: Nicola Bonora, Umberto Galietti, Luigi Bruno, Davide Castagnetti, Cristiana Del Prete, Mario Guagliano and Vigilio Fontanari

Published: 25 March 2026

caused by sensor installation, the high cost and complexity of instrumentation, sensor durability issues in operational environments and difficulties with in situ calibration. These challenges necessitate the use of indirect load estimation techniques. The inverse identification of dynamic loads is a common challenge in many engineering fields, including engine-induced vibrations [6,7], moving loads on bridges [8–10], wind-induced vibrations [11,12], and railroad applications. This is essentially an inverse problem in structural dynamics [13]. In the indirect approach, easily measurable quantities like deformations or displacements are recorded, and a linear relationship is established between these measurements and the applied loads [14–16]. Strain gauges present a cost-effective solution for this purpose. The technique of using strain measurements to reconstruct dynamic loads is known as load identification or reconstruction. In-service loads are linearly correlated with measured strains via a strain transfer matrix, derived numerically (e.g., through FE analysis), experimentally, or analytically. However, applying this technique is non-trivial. While optimal strain gauge number and placement are straightforward for simple structures, they become critically complex for intricate designs, where poor selection can lead to significant errors. This research aims to develop a methodology for automatically identifying the optimal positions and orientations for a strain gauge array used in load reconstruction. An overview of the load reconstruction method will be provided, followed by a detailed explanation of the proposed methodology. A numerical validation will then demonstrate the method's effectiveness, highlighting its potential for industrial applications on physical machines and structures.

2. Load Identification Methodology

The well-established methodology of load identification (or reconstruction) is applied to static linear elastic problems and is extensively discussed in [14–16] and in [17–19]. The term *linear* in this context implies that the strain response is proportional to the applied loading, as illustrated in Figure 1, even though certain portions of the structure may exhibit non-linear behavior, such as: local yielding near welds, bolted joints, or boundary conditions undergoing a non-linear strain response.

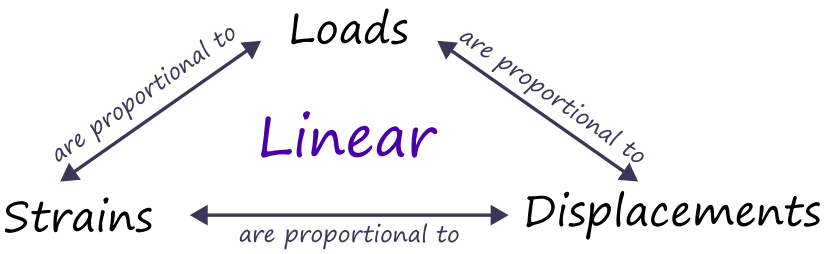

Figure 1. Linear material behavior schematic [15].

Provided the stress does not exceed the material's proportional limit and the structure remains stable such that the principle of superposition holds, the strain at any location on the structure can be expressed as a linear combination of the strains produced at that location by each load applied individually. This leads to a system of linear equations, which can be expressed in matrix form as follow:

$$\{\mathbf{S}\} = [\mathbf{A}]\{\mathbf{L}\} + \{\boldsymbol{\varepsilon}\} \quad (1)$$

where $\{\mathbf{S}\}$ is an $n \times 1$ vector of strains measured at n locations, representing the acquired experimental data; $[\mathbf{A}]$ is an $n \times p$ matrix (denoted as the strain transfer matrix) of sensitivity coefficients a_{ij}, relating the strain at location i due to a unit load applied at j; and $\{\mathbf{L}\}$ is a $p \times 1$ vector of generalized loads (forces or moments) at p locations, representing the

unknown quantities to be determined. Assuming $\{\mathbf{S}\}$ is measured and $[\mathbf{A}]$ is known, the least squares estimate of the unknown load vector $\{\mathbf{L}\}$ is given by:

$$\hat{\mathbf{L}} = (\mathbf{A}^{\mathrm{T}}\mathbf{A})^{-1}\mathbf{A}^{\mathrm{T}}\mathbf{S} \tag{2}$$

provided that $(\mathbf{A}^{\mathrm{T}}\mathbf{A})^{-1}\mathbf{A}^{\mathrm{T}}$, known as the Moore–Penrose pseudoinverse, exists. The hat notation, $\hat{\mathbf{L}}$, denotes an estimate of the parameter vector $\mathbf{L}$. Note that, in general, a number of strain gauges greater than the number of loads to be identified is required. Consequently, the resulting strain transfer matrix $[\mathbf{A}]$ is rectangular, and its inverse cannot be computed directly but must be estimated via the Moore–Penrose pseudoinverse. Furthermore, let $\{\varepsilon\}$ represent an $n \times 1$ vector of measurement errors associated with each strain gauge. If the strain measurement errors are independently and identically distributed with standard deviation σ, the variance-covariance matrix of the errors can be expressed as $\sigma^2\mathbf{I}$, where:

$$\sigma^2 = \frac{n\varepsilon^2}{(n-p)} \tag{3}$$

with n being the number of strain gauges and p the number of loads to be identified. The variance serves as a measure of the precision of the load estimates. The variance–covariance matrix for the load estimates is given by:

$$\mathrm{var}(\hat{\mathbf{L}}) = (\mathbf{A}^{\mathrm{T}}\mathbf{A})^{-1}\sigma^2 \tag{4}$$

The diagonal entries of this matrix represent the variances of the individual load estimates, while the off-diagonal terms correspond to the covariances between them. Smaller variances indicate higher precision in the load estimates. Thus, minimizing the uncertainty in the load estimates requires ensuring that the matrix $(\mathbf{A}^{\mathrm{T}}\mathbf{A})^{-1}$ is well-conditioned.

Practical Solution Procedure

The following outlines the procedure for reconstructing dynamic loads applied to a structure using time-varying strain data acquired from an array of sensors mounted on it.

i. Construct a finite element model of the component under investigation. Perform a series of static analyses equal to the number of loads to be identified. Forces (or moments) must be applied individually in the finite element model at the exact locations where the generalized loads are to be reconstructed.
ii. For each load case, extract the corresponding strain map of the component.
iii. Utilize the strain field information to determine, first, the number of strain gauges required (at minimum, equal to the number of loads to be identified) and, second, the optimal locations and orientations for the strain gauges. It is critical that the positions of the virtual gauges in the numerical model match those on the physical component as closely as possible. Misalignment in gauge positioning will introduce noise and errors into the load reconstruction process.
iv. Based on the number, location, and orientation of the gauges defined in the previous step, extract, from the FE analyses, the strain transfer matrix $[\mathbf{A}]$ required for the method.
v. Conduct experimental tests on the instrumented component to acquire the time-varying strain histories necessary for load identification. This provides the $\{\mathbf{S}\}$ vector for each time step.
vi. Using the known strain transfer matrix $[\mathbf{A}]$ and the measured strain histories, estimate the in-service loads acting on the component by applying Equation (2).

A complete flow chart of the approach is provided in Figure 2.

https://doi.org/10.3390/engproc2026131003

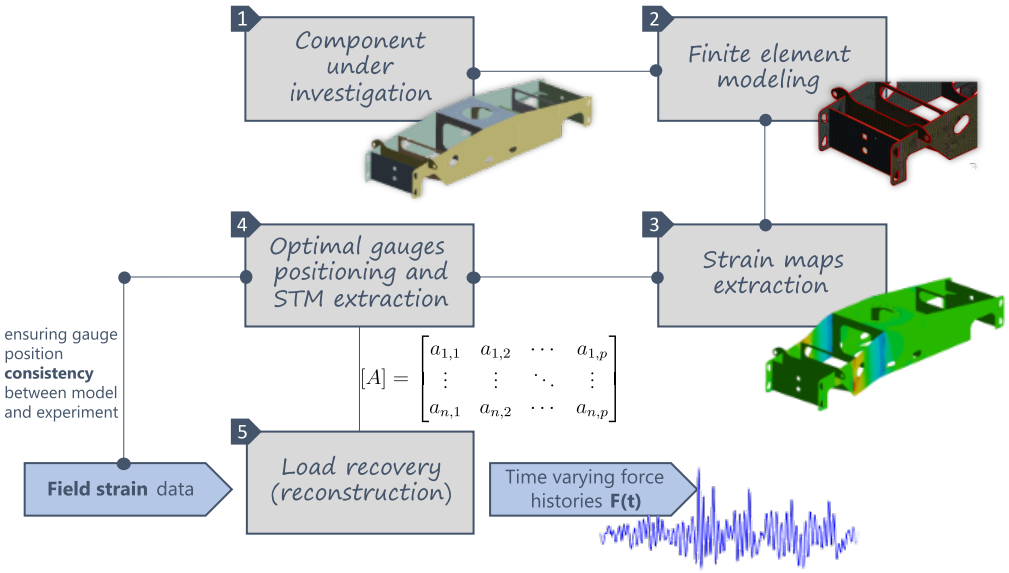

Figure 2. Flowchart illustrating the overall solution methodology. Load reconstruction can be performed by executing steps 1 through 5, in sequence.

3. Gauge Placement Problem

Following the procedure summarized in Figure 2, it is relatively easy to reconstruct the component in-service loads for further structural analysis. However, achieving an accurate reconstruction requires ensuring that the strain transfer matrix is well-conditioned. Theoretically, this matrix should be diagonal, a condition achieved when each strain gauge, whether virtual (on the FEM model for matrix extraction) or physical (on the actual structure), is positioned to be sensitive primarily to a single load condition. This ensures that the measurements are independent and non-redundant [20,21]. This independence is critical to prevent noise amplification within the matrix, which would otherwise lead to significant errors and invalid results. Furthermore, while it is often suggested in the literature to use a larger number of gauges, with respect to the loads that must be identified, to enrich the information within the strain transfer matrix, this approach can easily compromise the independence of the measurements if not executed carefully. Therefore, the principle of ensuring gauge independence is not merely a theoretical ideal but a fundamental practical necessity to obtain correct and usable results. Generally, the positions and orientations of strain gauges can be selected manually. For simple structures, such as the example shown in Figure 3, and a limited set of loads to identify, this approach can yield optimal results efficiently.

It is straightforward to observe that for a load applied along the Y-axis, gauge SG_1 provides the strongest response, while SG_2 theoretically remains unstrained, and vice versa for a load along the X-axis. However, for complex structures and a high number of loads to reconstruct, the manual selection process becomes highly subjective, prone to human error, and time consuming. Therefore, this work aims to develop an automated selection process to determine the optimal positions and orientations for all strain gauges involved in the analysis. The process, outlined below and highlighted in Figure 4, represents step n. 4 of the flow shown in Figure 2.

i. The application of the method requires the extraction of both the global strain maps and the stress tensor for each element and for each analyzed loading condition.
ii. The resulting list of elements can be filtered to remove those located in areas where physical strain gauge installation is impractical. Such areas include those affected by boundary conditions, weldments, or bolted joints. (The engineers performing the analysis must be aware of these constraints.)

https://doi.org/10.3390/engproc2026131003

iii. For each element and load condition, the determinant of the stress tensor is calculated. The resulting values are then sorted from highest to lowest, highlighting the structural regions subjected to the greatest stresses. These areas are therefore the most suitable candidates for strain gauge placement.

iv. The orientation is defined within the local element reference frame by selecting the direction (σ_{xx} or σ_{yy}) with the higher stress magnitude. This selection is limited to these two components because surface-mounted strain gauges only capture a plane stress state. This orientation can subsequently be redefined with respect to the global reference frame.

v. A second filtering step is then applied to maximize the probability of measurement independence across the set of strain gauges. If an element is identified as an optimal candidate location for more than one load case, it is automatically removed from the list.

vi. The final result provides the optimal locations and orientations for the entire set of strain gauges that must apply on the surface structure and also the strain transfer matrix that has to be used.

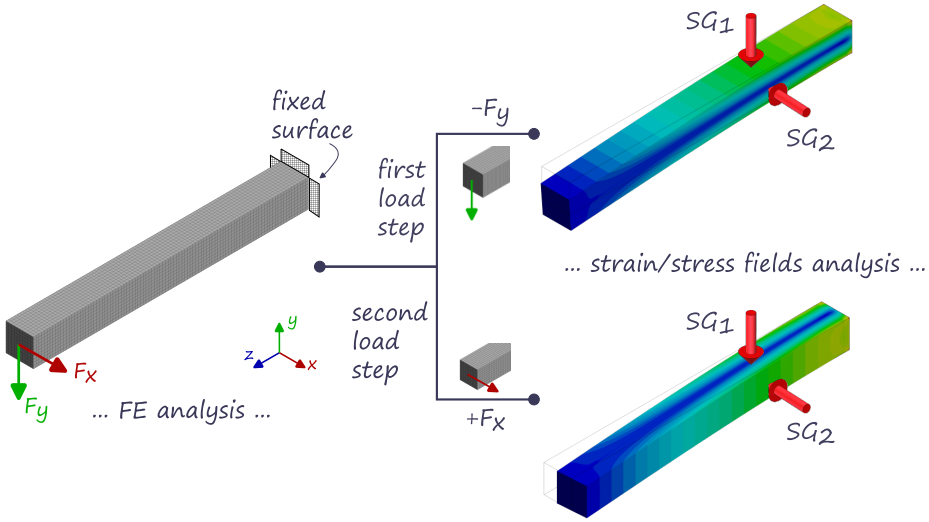

Figure 3. Manual strain gauge placement and orientation. The red arrows on the right side of the figure indicate two strain gauges potential positions to reconstruct loads along the directions corresponding to the two load steps.

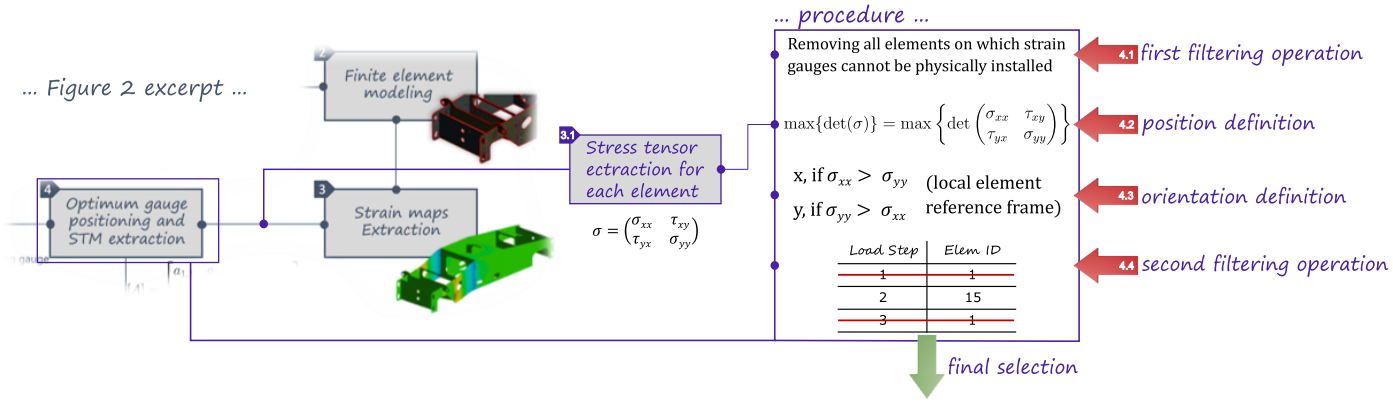

Figure 4. Automated selection method developed. Step 4 of Figure 2 is here expanded and the procedure explained from steps 4.1 through 4.4.

https://doi.org/10.3390/engproc2026131003

4. Validation

Due to the lack of experimental data for the specific structure under investigation, the schematized process in Figure 4 was numerically validated using the test case presented in Figure 5.

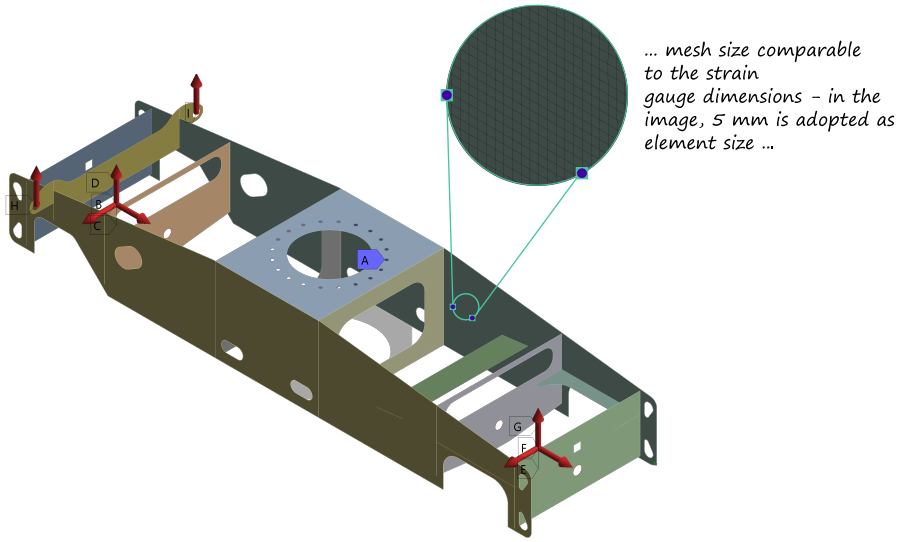

Figure 5. Test case adopted for process validation. Each red arrow represents a load step in the finite element analysis (FEA). The mesh element size is shown in the zoomed excerpt of the structure.

This structure represents the drive chassis of an aerial work platform, for which the dynamic loads acting in the directions indicated by the red arrows must be identified. Each arrow corresponds to a single load step in the Finite Element Analysis (FEA), conducted using Ansys® Mechanical, Release 24.2. The entire model was meshed with shell elements, with a maximum element size not exceeding the dimensions of the strain gauges that could be installed on the component surface for experimental measurements (Figure 5). This constraint was applied to avoid errors introduced by strain approximations. Following the methodology: (i) all static structural analyses were first solved to obtain the strain and stress fields for all the required loading conditions; (ii) the data were then extracted from the FE software (Ansys® Mechanical, Release 24.2) and processed according to the schematic in Figure 4, described in the previous section. This processing was accomplished using a custom-developed Python package (v3.12.2), LoadGauge, which leverages standard libraries (numpy [22], scipy [23], matplotlib [24]) alongside customized routines. This analysis led to the identification of the optimal strain gauge positions, orientations and to the definition of the strain transfer matrix, $[\mathbf{A}]$, shown in Table 1.

Table 1. Output strain transfer matrix generated by the automated method and used for the load identification process.

n° LS	SG1	SG2	SG3	SG4	SG5	SG6	SG7	SG8
1	1.68×10^{6}	-1.25×10^{5}	-1.43×10^{6}	-1.13×10^{3}	-3.39×10^{3}	6.95×10^{3}	-1.23×10^{5}	1.47×10^{5}
2	-1.46×10^{5}	5.49×10^{5}	1.75×10^{4}	-1.43×10^{5}	-3.88×10^{5}	8.38×10^{2}	5.49×10^{5}	5.49×10^{5}
3	-2.25×10^{5}	-2.22×10^{5}	6.62×10^{6}	-1.14×10^{4}	-3.75×10^{4}	-1.52×10^{4}	-3.47×10^{5}	-9.27×10^{4}
4	-3.07×10^{2}	9.03×10^{2}	-5.97×10^{3}	-1.42×10^{6}	4.11×10^{4}	1.27×10^{6}	-3.17×10^{4}	3.35×10^{4}
5	1.92×10^{5}	-3.77×10^{5}	2.58×10^{5}	1.14×10^{5}	-1.29×10^{6}	1.54×10^{6}	-1.02×10^{4}	-7.44×10^{5}
6	2.44×10^{4}	-6.79×10^{4}	-6.47×10^{3}	8.24×10^{4}	1.31×10^{5}	-7.65×10^{6}	-1.29×10^{5}	-6.70×10^{3}
7	8.71×10^{4}	2.19×10^{4}	-1.51×10^{5}	-2.04×10^{1}	-4.65×10^{1}	6.32×10^{3}	2.95×10^{6}	1.56×10^{5}
8	8.57×10^{4}	2.12×10^{4}	1.49×10^{5}	-2.02×10^{1}	-4.62×10^{1}	-6.21×10^{3}	1.53×10^{5}	2.89×10^{6}

In the absence of experimental data, a multibody machine model was developed and its dynamic behavior was simulated using Adams®/View 2020. The drive chassis was modeled as a flexible body to more accurately capture its structural dynamics, using the same finite element model shown in Figure 5. This approach enabled the extraction of strain time histories from the simulation at locations corresponding to a hypothetical array of strain gauges on the physical structure. Furthermore, the software allows for the direct retrieval of forces and moments at the joint locations, which are the target points for the reconstruction of load time series (indicated by the red arrows in Figure 5).

Figure 6 illustrates the comparison between the reaction forces extracted from Adams and those reconstructed using the proposed approach, demonstrating a strong match. Similarly, Figure 7 shows the correlation between reconstructed and simulated forces, which aligns closely with the ideal condition, further confirming the reliability of the reconstruction method.

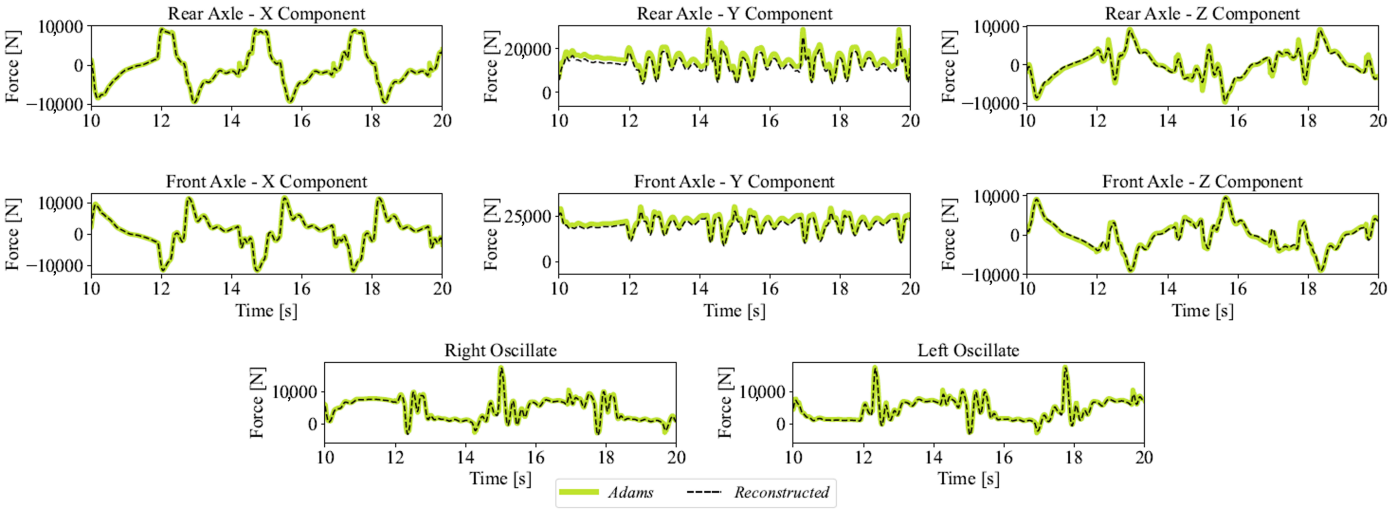

Figure 6. Comparison between reconstructed and simulated forces, showing strong agreement across all loading conditions and confirming the robustness of the adopted load reconstruction methodology.

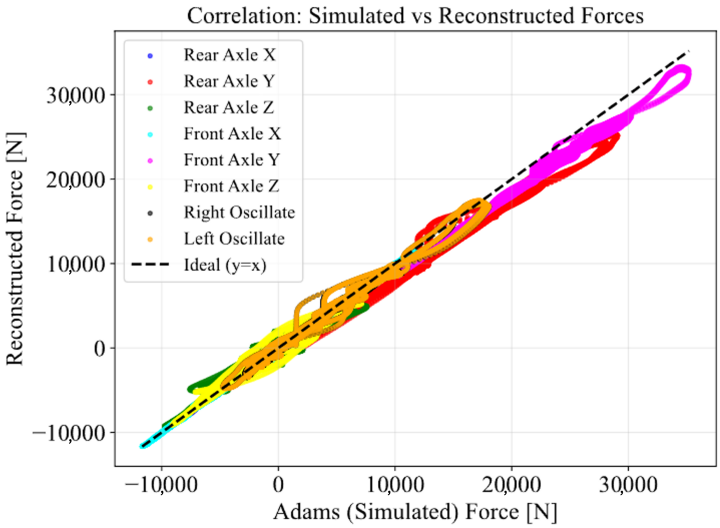

Figure 7. Correlation between reconstructed and simulated forces. Most graphs closely match the ideal condition, thereby validating the reconstruction approach.

5. Conclusions

This study successfully demonstrates the efficacy of a load reconstruction technique grounded in a well-posed, automated sensor placement strategy. The methodology proved

highly effective, yielding excellent results characterized by high-fidelity reconstructed load data. This output is sufficiently reliable to serve as input for advanced investigations, such as fatigue life analysis, structural optimization, or the development of a digital twin. A key advantage of the automated approach for strain gauge positioning and orientation is its ability to provide robust, optimal configurations while drastically reducing the engineering time typically required by traditional, iterative, and subjective manual selection processes. Furthermore, the algorithm's inherent structure is well-suited for parallel computing. Leveraging parallelization offers a clear pathway to significantly reduce computational timelines, thereby facilitating the application of this methodology to increasingly complex and detailed Finite Element Models for even more accurate analyses.

Author Contributions: Conceptualization, G.C. and M.P. and F.C.; methodology, G.C. and M.P.; software, G.C. and M.P. and F.C.; validation, G.C. and M.P.; resources, F.C.; data curation, G.C.; writing—original draft preparation, G.C.; writing—review and editing, G.C. and M.P.; supervision, F.C.; project administration, F.C. All authors have read and agreed to the published version of the manuscript.

Funding: This research received no external funding.

Institutional Review Board Statement: Not applicable.

Informed Consent Statement: Not applicable.

Data Availability Statement: Data will be made available on request.

Conflicts of Interest: Author Giacomo Cangi is employed by the Terex Italia S.r.l. The remaining authors declare that the research was conducted in the absence of any commercial or financial relationship that could be construed as a potential conflict of interest.

References

1. Chang, X.; Yan, Y.; Wu, Y. Study on solving the ill-posed problem of force load reconstruction. *J. Sound Vib.* **2019**, *440*, 186–201. [CrossRef]
2. Wickham, M.J.; Riley, D.R.; Nachtsheim, C.J. Integrating Optimal Experimental Design into the Design of a Multi-Axis Load Transducer. *J. Eng. Ind.* **1995**, *117*, 400–405. [CrossRef]
3. Gund, K.K.; Gore, S.R.; Patane, P.M.; Kate, H.R.; Lokhande, P.Z. Reconstruction of load histories using strain gauges. *Int. J. Curr. Eng. Technol.* **2017**, 100–104.
4. Cangi, G.; Angeletti, A.; Palmieri, M.; Cianetti, F. A Multibody Mathematical Model to Simulate the Dynamic Behavior of Aerial Work Platforms Using Python. *Eng. Proc.* **2025**, *85*, 36. [CrossRef]
5. Cianetti, F.; Garzia, R.; Palmieri, M.; Ambrogi, F.; Braccesi, C. An estimation model of suspension loads in explicit multibody simulation. *IOP Conf. Ser. Mater. Sci. Eng.* **2021**, *1038*, 012042. [CrossRef]
6. Van Herbruggen, J.; van der Linden, P.J.G.; Knittel, H.J.; Schnur, J. Engine Internal Dynamic Force Identification and the Combination with Engine Structural and Vibro-Acoustic Transfer Information. *SAE Trans.* **2001**, *110*, 2026–2032.
7. Leclère, Q.; Pezerat, C.; Laulagnet, B.; Polac, L. Indirect measurement of main bearing loads in an operating diesel engine. *J. Sound Vib.* **2005**, *286*, 341–361. [CrossRef]
8. Zhu, X.; Law, S. Moving loads identification through regularization. *J. Eng. Mech.* **2002**, *128*, 989–1000. [CrossRef]
9. Lee, S.Y. An Advanced Coupled Genetic Algorithm for Identifying Unknown Moving Loads on Bridge Decks. *Math. Probl. Eng.* **2014**, *2014*, 462341. [CrossRef]
10. Law, S.S.; Zhu, X.Q. *Moving Loads—Dynamic Analysis and Identification Techniques*; Structures and Infrastructures Book Series; CRC Press: Boca Raton, FL, USA, 2011; Volume 8.
11. Chen, T.C.; Lee, M.H. Inverse active wind load inputs estimation of the multilayer shearing stress structure. *Wind Struct.* **2008**, *11*, 19–33. [CrossRef]
12. Amiri, A.K.; Bucher, C.; Hoeffer, R. A practical procedure for inverse wind load reconstruction from different response types for large degrees of freedom structures. In *Proceedings of ISMA2016 Including USD2016*; Katholieke Universiteit Leuven: Heverlee, Belgium, 2016.
13. Nieminen, V.; Tuohineva, A.; Autio, M. Wheel load reconstruction using strain gauge measurements on the bogie frame for strain prediction and fatigue assessment. *Int. J. Fatigue* **2023**, *170*, 107533. [CrossRef]

14. Dhingra, A.K.; Hunter, T.G.; Gupta, D.K. Load Recovery in Components Based on Dynamic Strain Measurements. *J. Vib. Acoust.* **2013**, *135*, 051020. [CrossRef]
15. Hunter, T. Two-Wheeled Scooter Dynamics: Strains and Load Reconstruction. Available online: https://simutech.com.tw/uploads/products/trueload/nafems.pdf?srsltid=AfmBOoolX5vUkEbv8oVVLXdCdxURD5V0PHSI18qIItap387u5Tsz6FJD (accessed on 1 March 2026).
16. Wickham, M.J.; Galliart, D.R.; Nachtsheim, C.J.; Riley, D.R. *The Design and Application of a Multi-Axis Load Transducer*; SAE Technical Paper 940250; SAE International: Warrendale, PA, USA, 1994. [CrossRef]
17. Rathanraj, K.J.; Verma, A.K.; Srividya, A.; Mannikar, A.V.; Pankhawala, V.A. *Extrapolation of Service Load Data*; SAE Technical Paper 2009-01-1619; SAE International: Warrendale, PA, USA, 2009. [CrossRef]
18. Augustine, P.; Hunter, T.; Sievers, N.; Guo, X. *Load Identification of a Suspension Assembly Using True-Load Self Transducer Generation*; SAE Technical Paper 2016-01-0429; SAE International: Warrendale, PA, USA, 2016. [CrossRef]
19. Conle, F.A.; Chernenkoff, R.A.; Zhang, Y.; Chu, C.C.; Barrie, W. *Using Superposition to Calculate Critical Location Stress, Strain and Life in Vehicular Transmission Shafts of Complex Geometry Subjected to Bending and Torsion*; SAE Technical Paper 2002-01-1302; SAE International: Warrendale, PA, USA, 2002. [CrossRef]
20. Lourens, E.; Reynders, E.; De Roeck, G.; Degrande, G.; Lombaert, G. An augmented Kalman filter for force identification in structural dynamics. *Mech. Syst. Signal Process.* **2012**, *27*, 446–460. [CrossRef]
21. Da Luz, D.K.; Gertz, L.C.; Cervieri, A.; Rodrigues, A.F.A.; Da Silveira, M.A.; De Almeida, R.G.M. *Project of a Load Cell for a Dynamometer*; SAE Technical Paper 2010-36-0285; SAE International: Warrendale, PA, USA, 2010. [CrossRef]
22. Harris, C.R.; Millman, K.J.; van der Walt, S.J.; Gommers, R.; Virtanen, P.; Cournapeau, D.; Wieser, E.; Taylor, J.; Berg, S.; Smith, N.J.; et al. Array Programming with NumPy. *Nature* **2020**, *585*, 357–362. [CrossRef] [PubMed]
23. Virtanen, P.; Gommers, R.; Oliphant, T.E.; Haberland, M.; Reddy, T.; Cournapeau, D.; Burovski, E.; Peterson, P.; Weckesser, W.; Bright, J.; et al. SciPy 1.0: Fundamental Algorithms for Scientific Computing in Python. *Nat. Methods* **2020**, *17*, 261–272. [CrossRef] [PubMed]
24. Hunter, J.D. Matplotlib: A 2D Graphics Environment. *Comput. Sci. Eng.* **2007**, *9*, 90–95. [CrossRef]